VALIDATION OF A NEW NONLINEAR HEMT MODEL BY INTERMODULATION CHARACTERIZATION

Guoli Qu and Anthony E. Parker
Electronics Department, Macquarie University, Sydney Australia 2109

ABSTRACT

A new HEMT model is presented. The second and third-order intermodulation products of HEMT amplifiers are investigated at low frequency (50 MHz) and high frequency (1 GHz) respectively. Simulations performed with SPICE agree well with measurements. The contribution of nonlinear capacitance to intermodulation distortion is investigated.

INTRODUCTION

Nonlinear simulation of active circuits is important for microwave circuit design. For HEMT models, the main concern is the nonlinearity of the drain-source current and terminal capacitances. A new nonlinear drain-source current model for SPICE proposed in [1] features high-order continuity in the drain current description and its derivatives. This feature is important for correct simulation of intermodulation (IM) products, which are determined by the derivatives [2][3][4]. The aim of this paper is to extend the dc model of [1] to microwave frequency by adding a new capacitance model and to examine the validity of the model for predicting output power spectrum characteristics and intermodulation. A capacitance description is proposed, which based on our continuous 2-dimensional electron gas (2DEG) charge density model. The contribution of nonlinear capacitance to IM distortion is investigated.

Distortion measurements made at approximately 50 MHz using the high dynamic range RF TDFD technique [5] were used to confirm the accuracy of the dc model. Because device capacitance is insignificant at this frequency, this check establishes the validity of the drain current model alone. Distortion measurements repeated at 1 GHz were used to confirm the accuracy of the model at microwave frequency. Excellent agreement between simulated and measured intermodulation is demonstrated at both low frequency and high frequency. The model has been implemented in SPICE3F4.

NONLINEAR HEMT MODEL

The dc model proposed in [1] is used here as the basis for this study. This section briefly describes this dc model and the capacitance models that have been added to it.

DC Model In the linear region the dc model's drain current is described by a square law. In the saturation region the drain current is proportional to the HEMT's 2DEG density, n_s.

$$n_s(V_t) = \frac{cV_t^2}{1 + aV_t^2 + bV_t^3} \tag{1}$$

where a, b and c are constants and V_t is normally the gate potential V_g, but is restricted to a maximum value of $V_{so} = \sqrt[3]{2/b}$ by the following smooth transform controlled by parameter σ.

$$\begin{aligned} V_t &= \frac{1}{2}\sqrt{\left[V_g\sqrt{1+\sigma} + V_{so}\right]^2 + \sigma V_{so}^2} \\ &\quad -\frac{1}{2}\sqrt{\left[V_g\sqrt{1+\sigma} - V_{so}\right]^2 + \sigma V_{so}^2} \end{aligned} \tag{2}$$

The gate potential V_g is given by

$$V_g = V_{gt} - V_{cs} \tag{3}$$

where V_{cs} is the channel-source potential and V_{gt} is given by

$$V_{gt} = V_{ST} \cdot \ln\left[1 + \exp\left(\frac{V_{gs} - V_{TO}}{V_{ST}}\right)\right] \tag{4}$$

which implements subthreshold conduction characteristics. The terms a, b, σ, V_{ST} and V_{TO} are model parameters.

0-7803-4471-5/98/$10.00 (c) 1998 IEEE

Capacitance Model The capacitance model is based on a description of total charge. It is similar to the model described by [6] in which the charge under the gate, Q, in the linear operating region is assumed to be linearly distributed along the channel,

$$Q(V_{gs,}V_{gd}) = K_c\left(n_s(V_{ts}) + n_s(V_{td})\right) \tag{5}$$

where $K_c = \frac{qWL_e}{2}$, W and L_e are gate width and length respectively, V_{ts} is V_t given by (2) with V_{cs} set to zero, and V_{td} is V_t given by (2) with V_{cs} set to V'_{cs}:

$$V'_{cs} = \begin{cases} V_{ds} & V_{ds} < \left(2 - \frac{1}{\gamma}\right) V_{dss} \\ \left(1 - \frac{\left(1 - \frac{\gamma V_{ds}}{V_{dss}}\right)^2}{4\gamma(1-\gamma)}\right) V_{dss} & \text{otherwise} \\ V_{dss} & \frac{V_{dss}}{\gamma} < V_{ds} \end{cases} \tag{6}$$

In the linear region this function sets V'_{cs} equal to $V_{ds} = V_{gs} - V_{gd}$. In the saturated region this function models the independence of electron density at the drain end of the channel on V_{gd} by setting V'_{cs} equal to the drain-source saturation potential, V_{dss}. The parameter γ is a transition smoothing parameter ($0.5 < \gamma < 1$).

The gate-source capacitance, $C_{gs}(V_{gs}, V_{ds})$, is the partial derivative of Q with respect to V_{gs}, plus a fringing term $C_{gsp}(1 + n_{gs}V_{gs})$ [6],

$$\begin{aligned} C_{gs}(V_{gs}, V_{ds}) &= K_c\left(\frac{\partial n_s(V_{ts})}{\partial V_{gs}} + \frac{\partial n_s(V_{td})}{\partial V_{gs}}\right) \\ &\quad + C_{gsp}(1 + n_{gs}V_{gs}) \end{aligned} \tag{7}$$

where C_{gsp} and n_{gs} are model parameters.

The gate-drain capacitance, $C_{gd}(V_{gs}, V_{ds})$, is the partial derivative of Q with respect to V_{gd}, plus another fringing term $C_{gdp}(1 + n_{gd}V_{gd})$,

$$C_{gd}(V_{gs}, V_{ds}) = K_c\frac{\partial n_s(V_{td})}{\partial V_{gd}} + C_{gdp}(1 + n_{gd}V_{gd}) \tag{8}$$

where C_{gdp} and n_{gd} are model parameters.

MEASUREMENT AND SIMULATION

Measurements of intermodulation, with the TDFD technique [5], of ATF-36163 HEMTs in common-source configuration with 50Ω source and load impedances were performed. Simulations were performed with the model in [1] incorporating the capacitance model described in the previous section.

Low-frequency Results In the first instance, intermodulation measurements were made at frequencies less than 100 MHz, so that capacitance could be ignored. Figs 1, 2 and 3 show measured and simulated intermodulation as a function of gate-source bias, drain-source bias and input power, respectively. Two tones, 40 MHz and 59 MHz, were used for the RF TDFD measurement. The simulations coincide well with measurements, which confirms the accuracy of the dc model. All the parameters used in the simulations of Figs 1 (solid line), 2 and 3 were chosen to fit dc I/V characteristics. These include the access source and drain resistance $R_S = 3\ \Omega$, $R_D = 8\ \Omega$, which include the bias circuit.

The simulation of IM products as a function of V_{gs}, with all the parameters extracted from dc characteristic, coincides well with measurement at low gate-source potential. The fit is not so good at high gate-source potential, especially for IM2 as shown by the solid lines in Fig. 1. Simulation with reduced R_s significantly improved the agreement as shown by the dashed lines in Fig. 1. This drop of R_s at high frequency is expected and has been previously reported [7]. The notable decrease of the magnitude of parasitic source resistance R_s at microwave frequency results in an increase of the effective transconductance of HEMT [7].

High-frequency Results Next, the intermodulation measurements were repeated with a two-tone test at frequencies of 1.0 GHz and 1.1 GHz. Fig. 4 shows the measured and simulated output levels for a HEMT amplifier biased at $V_{ds} = 2.0$ V with an input power of –23 dBm per tone. The dc model parameters are the same as that used in the simulations at low frequency with reduced R_s. The parameters for the capacitance model ($C_{gsp} = 1$ pF, $C_{gdp} = 0.02$ pF, $n_{gs} = -0.9$, $n_{gd} = 0.1$ and $K_c = 1.6 \times 10^{-20}\mathrm{m}^2C$) were chosen to correctly predict the gain of the HEMT amplifier. Measurements and simulations agree well. The IM3 notch at high frequency, shown in Fig. 4 is shallower than that at low frequency shown in Fig. 1. This is because of the contribution of nonlinear capacitance.

Fig. 5 shows the simulated and measured output levels for the HEMT amplifier biased at $V_{gs} = -0.35$V with an input power of –23 dBm per tone. To investigate the contribution of nonlinear capacitance to IM products, simulations were compared with and without the nonlinear component in the capacitance model. To do this equations (7) and (8) can be written as

$$C_{gs} = \alpha\frac{\partial Q}{\partial V_{gs}} + C_{gsp}(1 + n_{gs}V_{gs}) \tag{9}$$

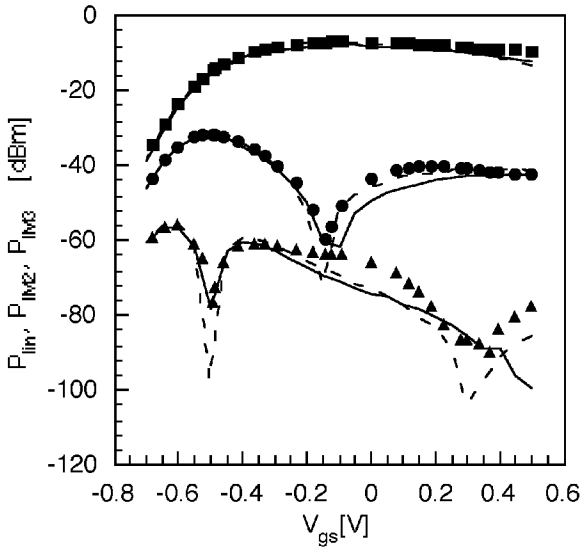

Figure 1: Simulated (lines) and measured fundamental (■), second-order (●), and third-order (▲) intermodulation levels as a function of V_{gs} for a HEMT amplifier biased at $V_{ds} = 2.0$ V. Input power is –23 dBm. Solid lines: simulation with the parameters selected by fitting dc I/V characteristics. Dashed lines: simulations with the same parameters as in solid line except access resistance R_s was reduced to 1.7 Ω.

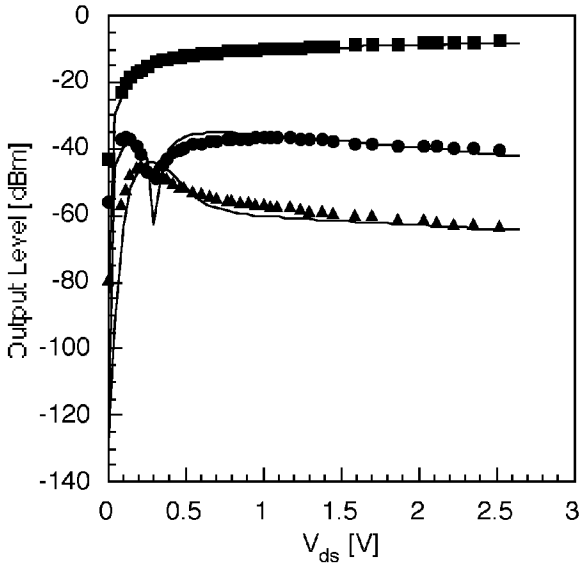

Figure 2: Simulated(lines) and measured fundamental (■), second- (●) and third- order (▲) intermodulation levels as a function of V_{ds} for a HEMT amplifier biased at $V_{gs} = -0.3$ V. Input level is –23 dBm.

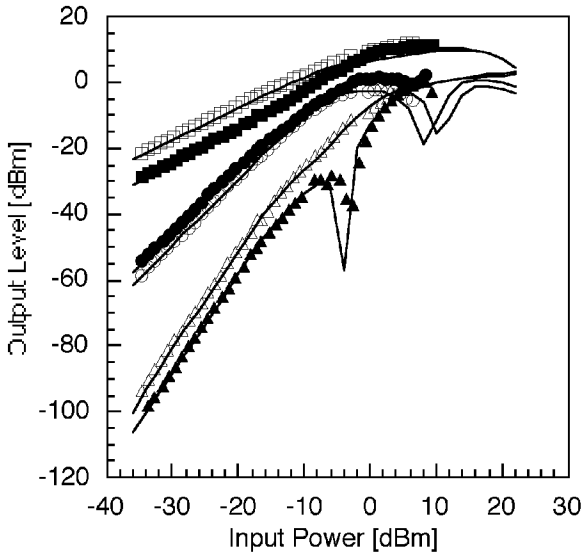

Figure 3: Simulated (lines) and measured fundamental (square) and second-order (circles), and third-order (triangles) intermodulation levels as a function of input power for a HEMT amplifier biased at $V_{gs} = -0.5$ V (solid symbols) and at $V_{gs} = -0.35$ V (open symbols). In both cases $V_{ds} = 2.0$.

$$C_{gd} = \alpha \frac{\partial Q}{\partial V_{gd}} + C_{gdp}(1 + n_{gd} V_{gd}) \qquad (10)$$

Firstly, simulations were performed without including any capacitance elements in the model. As expected, the simulations did not fit the high-frequency measurements.

Secondly, simulations were performed with a "linear capacitance model" by setting $\alpha = 0$ and $C_{gsp} = 1$ pF, $C_{gdp} = 0.02$ pF, $n_{gs} = -0.9$, $n_{gd} = 0.1$ in equations (9) and (10), which were chosen to fit the amplifier gain. Fundamental and the second-order distortion were predicted correctly. However the simulated third-order intermodulation level was much lower than the measurement, as shown by the dotted line in Fig. 5.

Thirdly, simulations were performed with the complete capacitance model using various levels of nonlinearity by setting $\alpha = 2$, $\alpha = 4$ and $\alpha = 8$ with $K_c = 8 \times 10^{-21} \mathrm{m}^2 C$ and all other parameters unchanged. Since the capacitance value of the nonlinear part in (7) and (8) was set very small, increasing them from $\alpha = 0$ to $\alpha = 8$ basically did not change the fundamental output as shown in Fig.5. The simulated second-order IM product did not exhibit any change either. However, the third-order intermodulation prod-

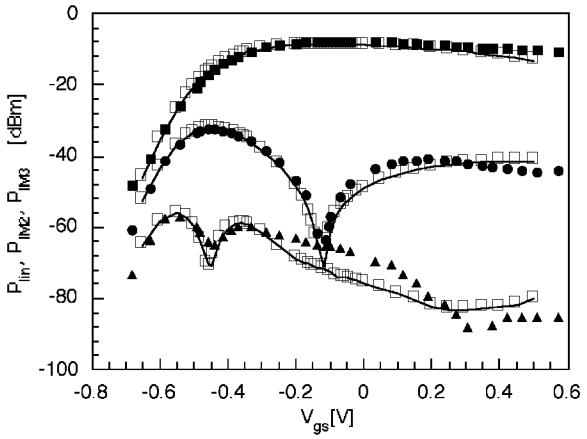

Figure 4: Measured high-frequency fundamental (■) second-order (●), and third-order (▲) intemodulation levels of a HEMT amplifier.

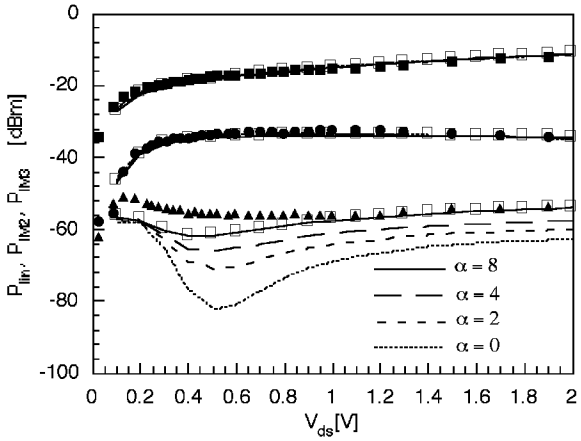

Figure 5: Simulated (lines) and measured high-frequency fundamental (■) second-order (●), and third-order (▲) intemodulation levels of a HEMT amplifier as a function of V_{ds} at $V_{gs} = -0.35$ V.

uct level is significantly increased with increased α and approaches measurement. This means that, at the frequency investigated, the nonlinearity of capacitance has significant contribution to the third-order intermodulation product, and not much to IM2. This agrees with Fig. 4 where IM3 notch is not as deep as that at low frequency. The notch has been filled in by capacitance nonlinearity.

CONCLUSION

The dc model proposed in [1] predicts intermodulation products over a wide range of bias and input levels very well. The accuracy of the model at high-frequency is confirmed by the agreement of measurements and simulations, which were performed with the dc model incorporating the capacitance model proposed in this paper.

At the frequency investigated, the capacitance has a more significant contribution to IM3 than to IM2. Careful characterization of the drain current description is most important for successful circuit simulation. As long as the drain-source current model predicts intermodulation distortion well at low frequency, the nonlinear distortion at high frequency can be predicted simply by incorporating with a nonlinear capacitance model.

ACKNOWLEDGMENTS

This work was funded by Macquarie University and the Australian Research Council. Ms Qu is supported by an Australian Overseas Postgraduate Research Scholarship.

*

References

[1] G. Qu and A. E. Parker, "Continuous HEMT model for SPICE," *IEE Electron. Lett.*, vol. 32, no. 14, pp. 1321-1323, July 1996.

[2] S. Maas and D. Neilson, "Modeling MESFET's for intermodulation analysis of mixers and amplifiers," *IEEE MTT-S Dig.*, pp. 1291-1294, 1990.

[3] G. Qu and A. E. Parker, "Analysis of intermodulation in HEMT common source amplifier," *The Proceedings of 6th International Symposium on Recent Advance in Microwave Technology*, pp. 243-246, August 1997, Beijing, China.

[4] G. Qu and A. E. Parker, "Modelling intermodulation distortion in MESFET/HEMTs," *The Proceedings of the 14th Australian Microelectronics Conference*, pp. 70-75, October, 1997, Melbourne, Australia.

[5] A. E. Parker and J. B. Scott, "Intermodulation nulling in GaAs MESFETs," *IEE Electron. Lett.*, vol. 29, no. 22, pp. 1961-1962, 1993.

[6] S. J. Mahon, D. J. Skellern, and F. Green, "A technique for modelling S-parameters for HEMT structures as a function of gate bias," *IEEE Trans. Microwave Theory Tech.*, vol. 40, no. 7, pp. 1430-1440, 1992.

[7] P. Roblin, S. Kang, A. Ketterson, and H. Morkoç, "Analysis of MODFET microwave characteristics," *IEEE Trans. Electron Dev.*, vol. 34, no. 9, pp. 1919-1927, Sept. 1987.